Article ID:0253-2778(2010)10-1023-06

Predicting the performance of microfluidic fuel cells

LU Zhaosheng[1], KONG Wei[2], LI Jiayu[2], CHEN Daifen[2],
DOU Xuan[1], WU Ping[1], HE Liqun[1]

(1. *Department of Thermal Science and Energy Engineering, University of Science and Technology of China, Hefei* 230027, *China*;
2. *Department of Physics, University of Science and Technology of China, Hefei* 230026, *China*)

Abstract: The performance of microfluidic-based fuel cells was predicted numerically by Fluent, where liquid fuel and liquid oxidant flow side by side in a channel at microscale and the current of electricity is achieved by electrochemical reactions at electrodes on channel walls. The obtained polarization curves were found to be in good agreement with experiments, and with the increase in the volumetric flow rate, the cell performance rises gradually. In our case, the cell performance is very sensitive to the content of oxygen in the cathode stream, while it is insensitive to the concentration of formic acid in the anode stream, confirming the cathode limited performance in microfluidic fuel cell as reported by others.

Key words: microfluidic fuel cell; polarization curve; simulation; FLUENT
CLC number: TM911.4 **Document code**: A doi:10.3969/j.issn.0253-2778.2010.10.006

微流体燃料电池性能的预测

卢照升[1],孔 为[2],李家玉[2],陈代芬[2],窦 轩[1],吴 平[1],何立群[1]

(1. 中国科学技术大学热科学与能源工程系,安徽合肥 230027;
2. 中国科学技术大学物理系,安徽合肥 230026)

摘要:报道了基于微流体技术的燃料电池性能的数值预测.在这种微流体燃料电池中,液态燃料和氧化剂并行流入微通道,电池的内部电流是微通道内离子的横向输运形成的.模型考虑了流体动力、组分的对流和扩散以及发生在电极表面的电化学反应.通过给定一组工作电压,利用FLUENT软件预测对应的电流密度.计算结果表明,计算得到的电池的极化曲线与实验结果吻合较好.随着反应物体积流率的增加,两股流体的混合程度降低,浓度边界层厚度明显减小,电池性能逐渐增加.电池性能对阴极流体中氧气浓度的变化比较敏感,而阳极流体中甲酸浓度的变化对其影响较小.这一计算结果表明这种微流体燃料电池是阴极受限的,这与实验结果一致.

关键词:微流体燃料电池;极化曲线;数值模拟;FLUENT

Received: 2010-05-20; **Revised**: 2010-10-13
Foundation item: Supported by National Natural Science Foundation of China (50876100).
Biography: LU Zhaosheng, male, born in 1984, master. Research field: microfludic fuel cell. E-mail: zslu@mail.ustc.edu.cn
Corresponding author: HE Liqun. PhD/associate Prof. E-mail: heliqun@ustc.edu.cn

0 Intruduction

A fuel cell is a device that can convert chemical energy to electricity by electrochemical reactions at its anode and cathode, which are connected by both an external circuit and the internal motion of ions through a membrane separating the two electrodes[1]. The fuel cells include proton exchange membrane fuel cell (PEMFC), direct liquid fuel cell (DLFC), and biofuel cell (BC)[2]. Recently, downsizing of fuel cells has been attracting more and more attention from researchers and industries for the potential use in portable devices, such as cell phones, laptop computers and MEMS systems[3]. However, the final size of such a fuel cell is found to be eventually determined by the membrane. Although increasingly smaller membranes are being found in labs, the microfluidic technology seems to be able to solve the membrane-related issues absolutely[4], where the fuel and oxidant flow through a microchannel in parallel and an ion can diffuse across their border to reach the other electrode. That is, there is no membrane between the two electrolyes. The proposed microfluidic fuel cells include T-, Y- or F-channel configurations[2].

To design such a fuel cell, a theoretical model is needed for predicting the performance of a microfluidic fuel cell. Bazylak et al[5] first conducted a computational study about T-shaped formic acid/ oxygen dissolved in sulfuric acid microfluidic fuel cells, where the fluid flows, species transports and chemical reactions were coupled and various cross-sections and electrode configurations were considered. Chang et al[6] coupled the Bulter-Volmer equation with the electric potential equation. Their numerical results showed that the cell's performance qualitatively was in good agreement with experiments, but the predicted potential for a known cell was always less than its experimental data. Chen et al[3] studied F-shaped membraneless fuel cells with the model. Ahmed et al[7] optimized the geometry to make full use of a fuel, and numerically analyzed a membraneless fuel cell designed by Cohen[8]. Here, we simulate the performance of a microfluidic fuel cell by Fluent, which gives current densities against a set of known working voltages instead of solving the electric field as usual.

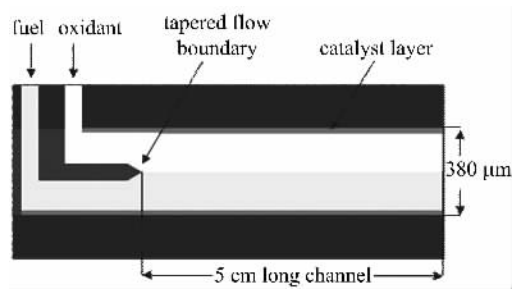

Fig. 1 Schematic representation of a microfluidic fuel cell

1 Government equation

The configuration of a microfluidic fuel cell is shown in Fig. 1. The length, width and height of the channel is 5 cm, 1 mm and 380 μm, respectively. In the microfluidic cell, the fuel refers to the formic acid in 0.1 mol/L sulfuric acid solution and the oxidant refers to the oxygen dissolved in a sulfuric acid solution of 0.5 mol/L. Electrochemical reactions are assumed to occur at the anode and cathode[5].

The reaction at the anode is

$$HCOOH \longrightarrow CO_2 + 2H^+ + 2e^- \quad (1)$$

The resulting electrons flowing through the external circuit and the protons diffusing through the solutions are supposed to meet at the cathode and react with oxygen as follows:

$$O_2 + 4H^+ + 4e^- \longrightarrow 2H_2O \quad (2)$$

In reality, there is not enough time for the protons created at the anode to diffuse to the cathode. The protons needed for the oxygen reduction reaction are provided by oxidant flow itself. The products of two reactions at the electrodes are removed by fluid flows. The system is assumed to be isothermal because the viscous dissipation is weak[5], and the fluid flow, ion diffusion and electrochemical reactions at

electrodes are described by continuity equation, Navier-Stokes equation of chemical reaction as well as convective-diffusion equation.

$$\nabla \cdot \boldsymbol{U} = 0 \tag{3}$$

$$\nabla \cdot (\boldsymbol{U}\boldsymbol{U}) = -\frac{1}{\rho}\nabla p + \nabla \cdot (\nu \nabla \boldsymbol{U}) \tag{4}$$

Where $\boldsymbol{U}$ is the velocity, ρ is the fluid density, p is the static pressure, and ν is the kinematic viscosity. The conservation of species equation is shown below,

$$\nabla \cdot (\rho Y_i \boldsymbol{U}) = -\nabla \cdot (\rho D_i \nabla Y_i) + M_i \cdot \frac{j_i}{n_i F} \tag{5}$$

where the subscript "i" represents the reactant species, Y is the local mass fraction, D is the diffusion coefficient, M is the mole mass, n is the number of electrons transferred in the reaction, F is the Faraday constant, and j is the local current density which also is the rate of electrochemical reaction. j_a and j_c are the current densities at the anode and cathode, and can be calculated by the Bulter-Volmer equation as below[7]:

$$j_a = j_{0,a}^{ref} \cdot \left(\frac{C_{HCOOH}}{C_{HCOOH}^{ref}}\right)^{\gamma_{HCOOH}} \cdot \left[\exp\left(\frac{\alpha n F}{RT}\eta_{act,a}\right) - \exp\left(-\frac{\alpha n F}{RT}\eta_{act,a}\right)\right] \tag{6}$$

$$j_c = j_{0,c}^{ref} \cdot \left(\frac{C_{O_2}}{C_{O_2}^{ref}}\right)^{\gamma_{O_2}} \cdot \left[\exp\left(\frac{\alpha n F}{RT}\eta_{act,c}\right) - \exp\left(-\frac{\alpha n F}{RT}\eta_{act,c}\right)\right] \tag{7}$$

where the subscript "c" represents the cathode and the subscript "a" represents the anode, j^{ref} is the exchange current density at the reference reactant concentration C^{ref}, γ is the reaction order, α is the charge transfer coefficient which is different at the anode and cathode, η_{act} is the activation overpotential, R is the universal gas constant, and T is the temperature.

At the cathode of Pt, the oxidation of formic acid needs two steps in series[5]:

$$Pt^0 + HCOOH \longrightarrow (COOH)_{ads} + H^+ + e^- \tag{8}$$

$$(COOH)_{ads} \longrightarrow CO_2 + H^+ + e^- + Pt^0 \tag{9}$$

The second step is found to be faster than the first one, so the reaction rate in the first step of dehydrogenation decides the overall rate of electron transfer, resulting in $n=1$ in Eq. (6).

Similarly, the oxygen is consumed as follows[10],

$$O_2 + H^+ + e^- \longrightarrow (OOH)_{ads} \tag{10}$$

$$(OOH)_{ads} + H_2O \longrightarrow 3(OH)_{ads} \tag{11}$$

$$(OH)_{ads} + H^+ + e^- \longrightarrow H_2O \tag{12}$$

The activation of reaction (10) is much higher than subsequent steps[11], so it is the critical step in terms of the overall rate of reaction, meaning $n=1$ in Eq. (7). Generally, the critical step is a first-order reaction, meaning $\gamma_{O_2} = 1$ and $\gamma_{HCOOH}=1$[5].

2 Numerical method

The numerical calculation aims to show the relationship of electrical current density at the surface of electrode with the working voltage. That is, current densities are predicted given a set of working voltages. The reported experiments show that the performance of a microfluidic fuel cell is cathode-limited. Usually, the activation of the anode is rather small as compared to that of the cathode, so we first give a guess on the activation of the anode and then calculate the activation of the cathode. Given working voltage of a fuel cell, the potential needed for activating the cathode[9] is

$$\eta_{act,c} = E_{Nernst} - V_{cell} - \eta_{conc,a} - \eta_{conc,c} - \eta_{ohmic} - \eta_{act,a} \tag{13}$$

E_{Nernst} is the maximal voltage as predicted by the Nernst equation in the following[1],

$$E_{Nernst} = E^0 - \frac{RT}{4F} \cdot \ln\left(\frac{\alpha_{CO_2}^2 \cdot \alpha_{H_2O}^2}{\alpha_{HCOOH}^2 \cdot \alpha_{O_2}}\right) \tag{14}$$

E^0 is reversible open voltage and α_i is the activity of species i.

The rest of the items in Eq. (13) are working voltage of the cell and its extra costs for low concentration at surfaces of two electrodes, the ohmic loss caused by ion transport resistance, electron transport resistance and contact resistance. After neglecting the accumulation of products at electrodes, their local concentration losses $\eta_{conc,c}$ and $\eta_{conc,a}$ are calculated as follows[1]:

$$\eta_{\mathrm{conc,c}} = \frac{RT}{4F} \cdot \ln\left(\frac{C_{\mathrm{O_2,b}} \cdot C^4_{\mathrm{H^+,b}}}{C_{\mathrm{O_2,s}} \cdot C^4_{\mathrm{H^+,s}}}\right) \quad (15)$$

$$\eta_{\mathrm{conc,a}} = \frac{RT}{2F} \cdot \ln\left(\frac{C_{\mathrm{HCOOH,b}}}{C_{\mathrm{HCOOH,s}}}\right) \quad (16)$$

where the subscript "b" represents the bulk and subscript "s" represents the surface of electrodes.

Given an activation of the anode, an activation of cathode can be obtained by Eq. (13), and the performance of a cell is obtained by a series of steps of this calculation. Because the currents through the anode and cathode are equal[9], the anode activation is updated in each step by the conservation in charge as follows,

$$I_{\mathrm{total}} = \sum_{i=1}^{N_c} j_{c,i} \cdot A_i = \sum_{i=1}^{N_a} j_{a,i} \cdot A_i \quad (17)$$

Where I_{total} is the total current from the anode to the cathode. N_c and N_a are the total numbers of mesh cells at the cathode and anode surface, each of which is of area A_i. In the process, the activations of two electrodes are different. Given a working voltage, the activations are updated after they have converged to their stable values. The iterative process for finding their stable values starts as each working voltage is given.

The computation is performed over a mesh of 400 000 hexahedron cells in Fluent. The fluid flow, mass transport and electrochemical reaction are solved simultaneously. In computation, the values of velocity and mass fraction of every species are given at the inlets of the micro-channel, and we choose pressure boundary conditions for both fuel and oxidant flows. Parameters used for computation are listed in Tab. 1. The working temperature is at $T = 298$ K and the reversible voltage is 1.48 V[6]. The effective density and viscosity of fuel and oxidant are weighted by mass ratios of each species.

3 Results and discussion

The numerical results for parameters in Tab. 1 are compared with experiment results in terms of their polarization curves (Fig. 2), and they are in good agreement with each other[8].

Tab. 1 Parameters used in anodic and cathodic flows

parameter	anode	cathode
inlet flow rate/(mL · min^{-1})	0.5	0.5
inlet reaction concentration/(mol · L^{-1})	0.5	1.25×10^{-3}
exchange current density/(A · m^{-2})	0.1194	3.1×10^{-7}
reference reaction concentration/(mol · L^{-1})	0.01	0.1
conductivity/(s · m^{-1})	5	4.78
diffusivity/(m^2 · s^{-1})	2.546×10^{-9}	2.1×10^{-9}
charge transfer coefficient	0.497	0.5
reaction order	1	1

The effect of volumetric flow rate on the performance of a microfluidic fuel cell is studied. We increase the flow rate of reactants in a hope to narrow the depletion zone above the electrode surface. As the concentration at surface is close to the bulk one, less and less energy is consumed on the diffusion of reactants to the surface. As shown in Fig. 3, the cell performance rises gradually with the flow rate. The variations of mass fraction of oxygen at outlet with four assigned volumetric

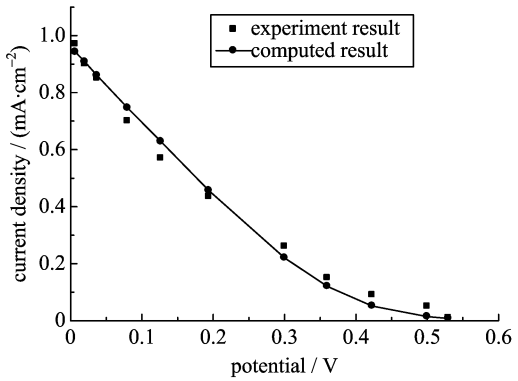

Fig. 2 Comparison of polarization curves: calculation vs experiment

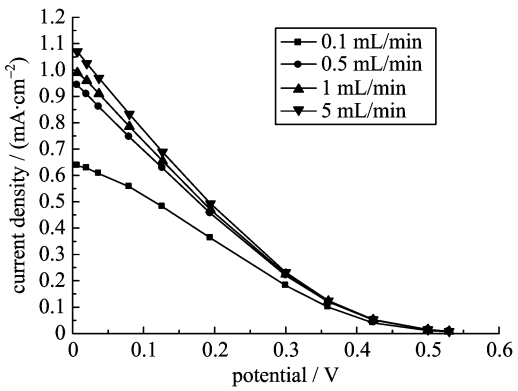

Fig. 3 The effect of volumetric flow rate on performance of a microfluidic fuel cell

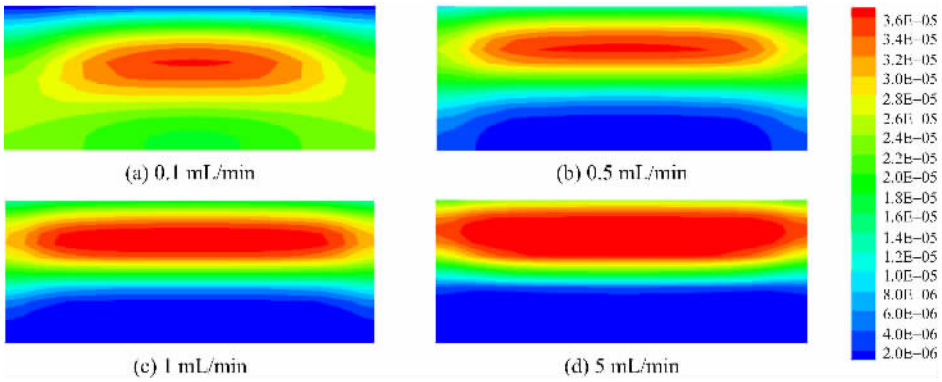

Fig. 4 The mass fraction of oxygen at outlet at four volumetric flow rates

flow rates are demonstrated in Fig. 4. When the flow rate is too low, the mixing of fuel and oxidant streams is rather serious and the depletion zone near the electrode's surface is more apparent. With the increase in the volumetric flow rate, the boundary layer of concentration above the cathode and the mixing of both streams decreases in thickness significantly, but the volumetric flow rate can't be always increased for some hydrodynamics instability would appear on some critical value[4,6].

The reported experiments[8] show that this sort of microfluidic fuel cell is cathode-limited, suggesting that any improvement to the cathode in reaction certainly leads to an increase of performance of such a fuel cell. To see the effects of oxygen concentration in cathode stream more clearly, we increase the concentration of supplied oxygen from 0.25 to 5 mmol/L when the flow rate is 0.5 mL/min, as shown in Fig. 5. The results indicate that the cell performance can be improved significantly at high oxygen concentrations, as shown in Fig. 5, confirming that the microfluidic fuel cell is cathode-limited as reported by others.

The cathode-limited behavior of the fuel cell may lie in the fact that the concentration of oxygen is much lower than that in formic acid. With the increase in oxygen concentration, the electro-catalytic activity of cathode can be enhanced, but the solubility (1～4 mmol/L) of oxygen limits the highest content[2,12]. More importantly, the oxygen diffusion (2×10^{-9} m^2/s) in the aqueous electrolyte limits the rate of replenishing the loss of oxygen on cathode[12]. These two aspects set the limit on performance of the microfluidic fuel cell. Jayashree et al[12] studied the air-breathing laminar flow-based microfluidic fuel cell with a GDE (gas diffusion electrode) as the cathode, and a better performance was obtained due to the diffusion coefficient (2×10^{-5} m^2/s) and content (10 mmol/L) of oxygen in air being higher than in aqueous media. Other oxidants were also used besides oxygen, such as H_2O_2[13], $KMnO_4$[4] and VO^{2+}[14].

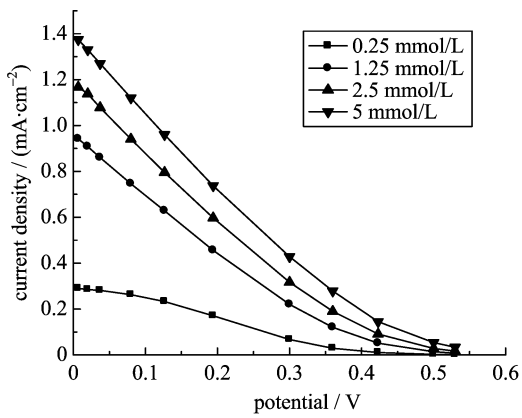

Fig. 5 The effect of oxygen concentration on the performance of microfluidic fuel cell

4 Conclusion

The voltage-current density of a microfluidic fuel cell can be solved without solving the electric field as usual, and the results are in good agreement with reported experimental data. The cell performance increases significantly at a high

volumetric flow rate and concentration of oxygen. The results demonstrate that the microfluidic fuel cell is distinct from its conventional counterpart in some aspects, such as the dominant role of convection over diffusion, and the ion transfer to the opposite electrode by crossing the interface. In this case, instead of the transport in an exchange membrane, the fluid boundaries near electrode surfaces become critical in cell performance. So a model specific to microfluidic fuel cells is needed as a tool to guide the design of such a fuel cell.

References

[1] O'hayre R, Cha S W, Colella W, et al. Fuel Cell Fundamentals[M]. New York: John Wiley & Sons, Ltd, 2006.

[2] Kjeang E, Djilali N, Sinton D. Microfluidic fuel cells: A review [J]. Journal of Power Sources, 2009, 186: 353-369.

[3] Chen F, Chang M H, Lin M K. Analysis of membraneless formic acid microfuel cell using a planar microchannel [J]. Electrochimica Acta, 2007, 52: 2 506-2 514.

[4] Choban E R, Markoski L J, Wieckowski A, et al. Microfluidic fuel cell based on laminar flow[J]. Journal of Power Sources, 2004, 128:54-60.

[5] Bazylak A, Sinton D, Djilali N. Improved fuel utilization in microfluidic fuel cells: A computational study [J]. Journal of Power Sources, 2005, 143: 57-66.

[6] Chang M H, Chen F, Fang N S. Analysis of membraneless fuel cell using laminar flow in a Y-shaped microchannel[J]. Journal of Power Sources, 2006, 159:810-816.

[7] Ahmed D H, Park H B, Sung H J. Optimum geometrical design for improved fuel utilization in membraneless micro fuel cell [J]. Journal of Power Sources, 2008, 185:143-152.

[8] Cohen J L, Westly D A, Pechenik A, et al. Fabrication and preliminary testing of a planar membraneless microchannel fuel cell[J]. Journal of Power Sources, 2005, 139:96-105.

[9] Nguyen P T, Berning T, Djilali N. Computational model of a PEM fuel cell with serpentine gas flow channels [J]. Journal of Power Sources, 2004, 130: 149-157.

[10] Antoine O, Bultel Y, Durand R. Oxygen reduction reaction kinetics and mechanism on platinum nanoparticles inside Nafion [J]. Journal of Electroanalytical Chemistry, 2001, 499: 85-94.

[11] Anderson A B, Roques J, Mukerjee S, et al. Activation energies for oxygen reduction on platinum alloys: Theory and experiment [J]. The Journal of Physical Chemistry B, 2005, 109: 1 198-1 203.

[12] Jayashree R S, Gancs L, Choban E R, et al. Air-breathing laminar flow-based microfluidic fuel cell [J]. J Am Chem Soc, 2005, 127:16 758-16 759.

[13] Kjeang E, Brolo A G, Harrington D A, et al. Hydrogen peroxide as an oxidant for microfluidic fuel cells [J]. Journal of the Electrochemical Society, 2007, 154: B1 220-B1 226.

[14] Kjeang E, Proctor B T, Brolo A G, et al. High-performance microfluidic vanadium redox fuel cell [J]. Electrochimica Acta, 2007, 52:4 942-4 946.